

An emerging Janus MoSeTe material for potential applications in optoelectronic devices

Xiaoyong Yang ^{a,b}, Deobrat Singh ^{b*}, Zhitong Xu ^a, Ziwei

Wang^a, and Rajeev Ahuja ^{b,c*}

^a National Collaborative Innovation Center for Nuclear Waste and Environmental Safety, Southwest University of Science and Technology, Mianyang 621010, China

^b Condensed Matter Theory Group, Materials Theory Division, Department of Physics and Astronomy, Uppsala University, Box 516, 75120 Uppsala, Sweden

^c Applied Materials Physics, Department of Materials and Engineering, Royal Institute of Technology (KTH), S-100 44 Stockholm, Sweden

*Corresponding author: deobratsingh9@gmail.com; Rajeev.ahuja@physics.uu.se

Fax: +46 184713524 Tel: +46 728772897

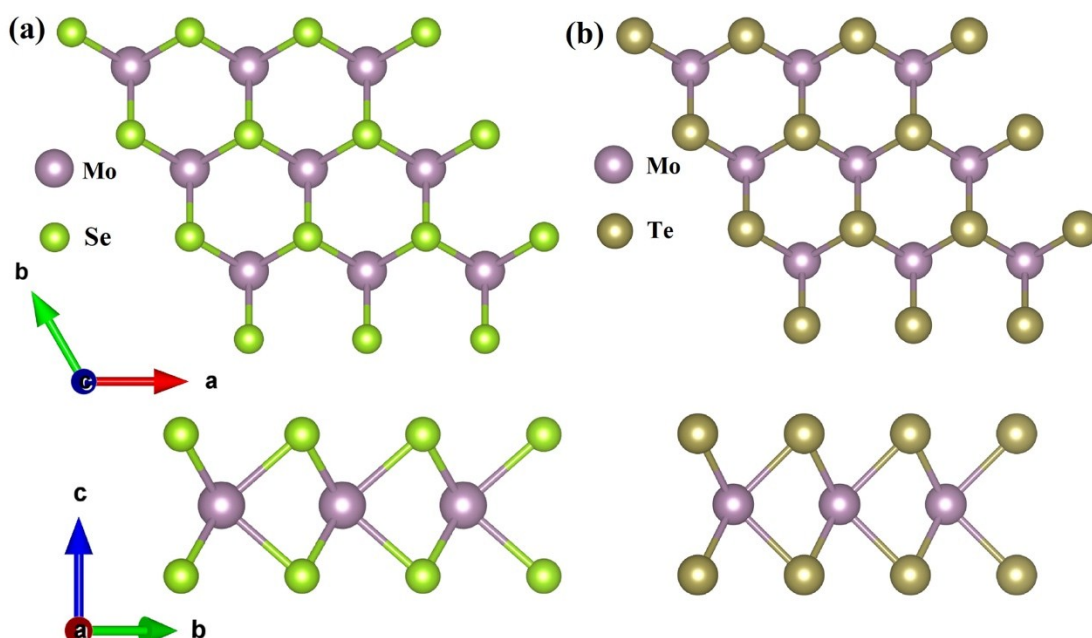


Figure. S1 Top (upper) and side (bottom) views of (a) MoSe₂ and (b) MoTe₂ in 2H phase. The purple, dark yellow, and green spheres are Mo, Te and Se atoms, respectively.

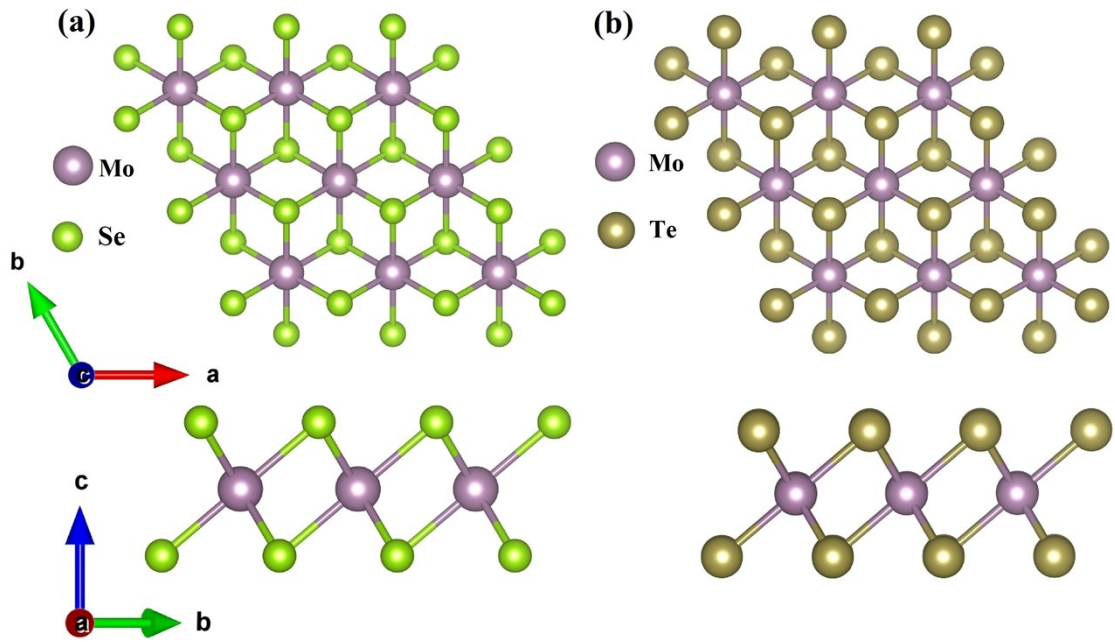


Figure. S2 Top (upper) and side (bottom) views of (a) MoSe₂ and (b) MoTe₂ in 1T phase. The purple, dark yellow, and green spheres are Mo, Te and Se atoms, respectively.

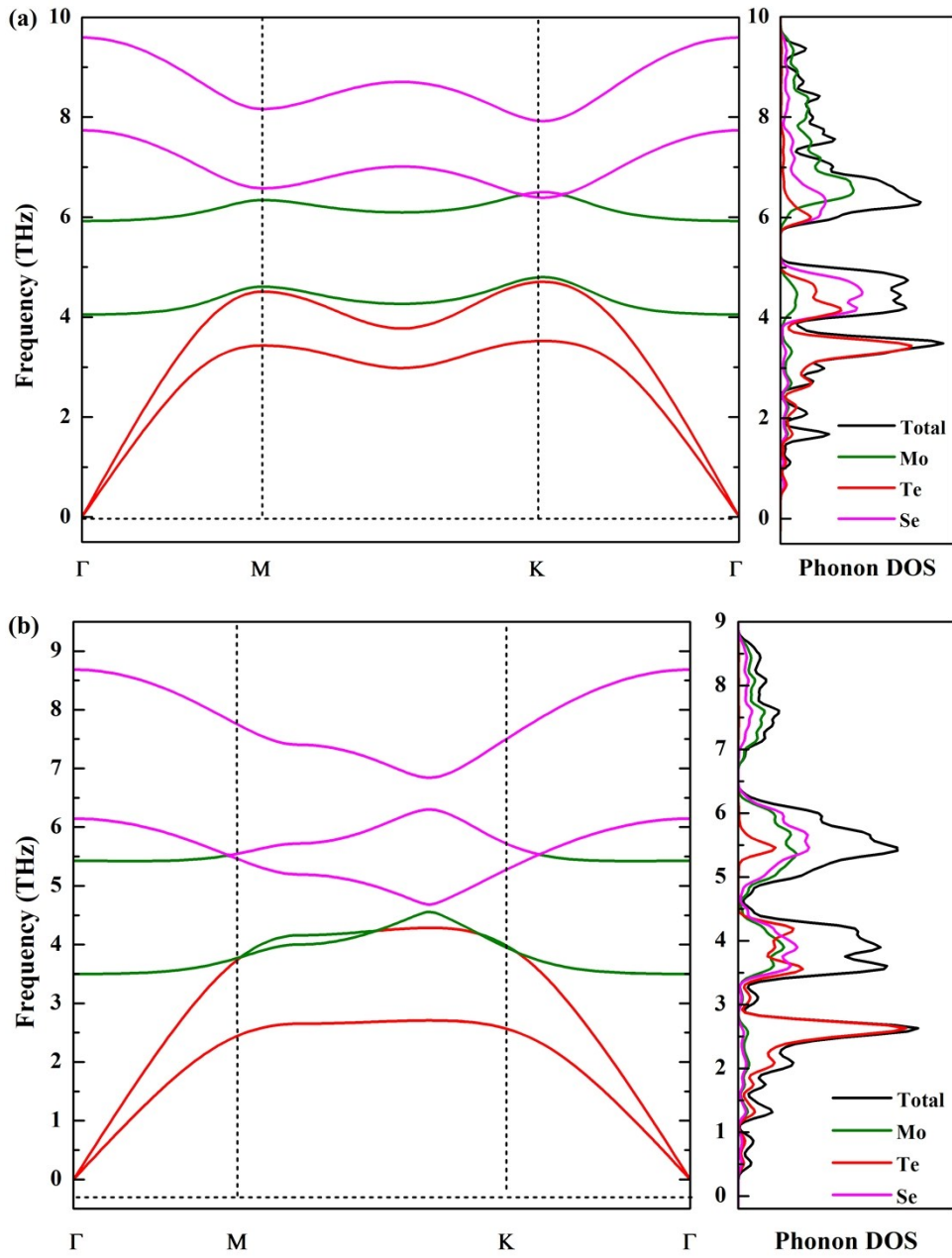


Figure. S3 The phonon dispersion and phonon density of Janus MoSeTe monolayer in (a) 2H and (b) 1T phases, respectively.

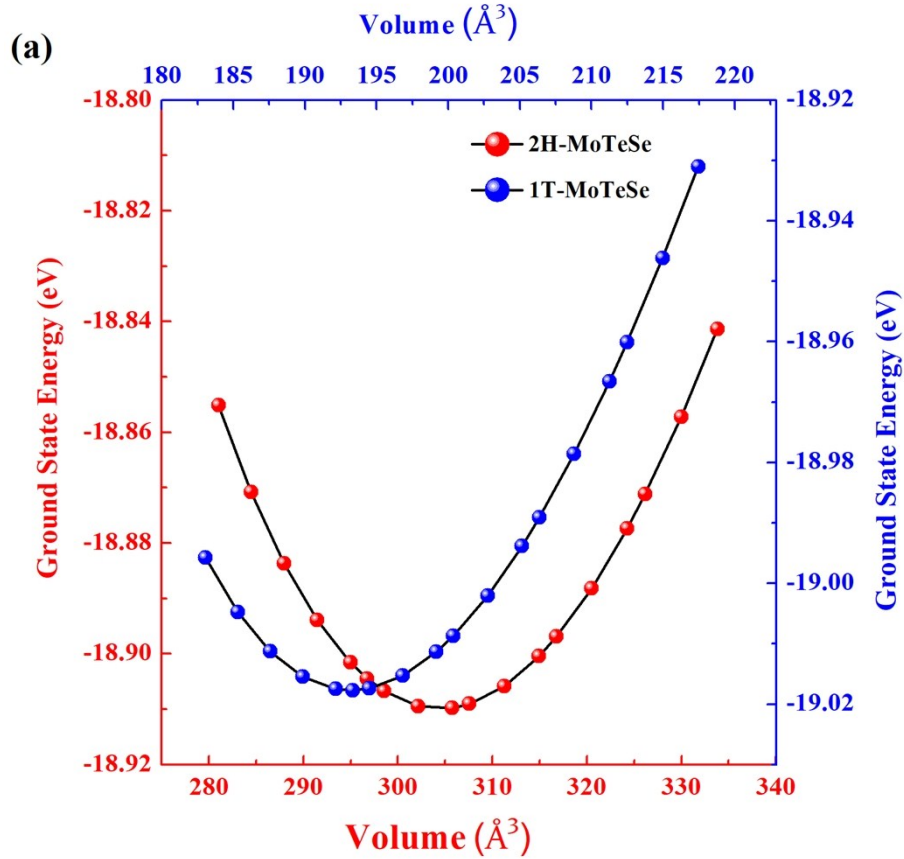


Figure. S4 The volume dependence of ground total energy for MoSeTe monolayer in 2H and 1T phases, respectively.

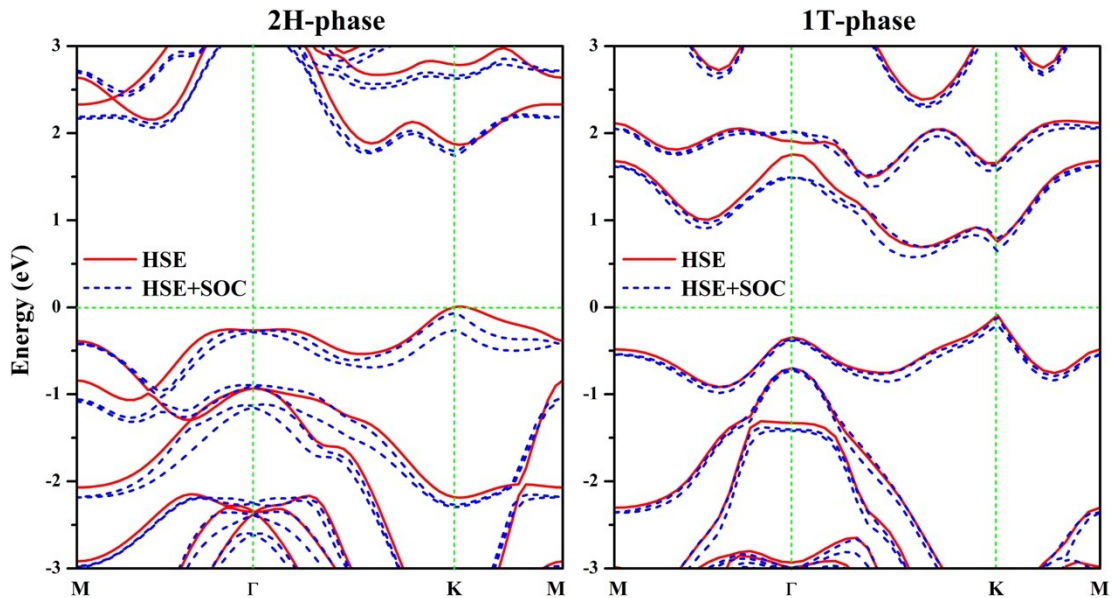


Figure. S5 Band structure of Janus MoSeTe monolayer in (a) 2H and (b) 1T phase, respectively, by using HSE (red solid lines) and HSE+SOC (blue dash lines) functions, respectively. The dotted lines indicate the position of the Fermi level.

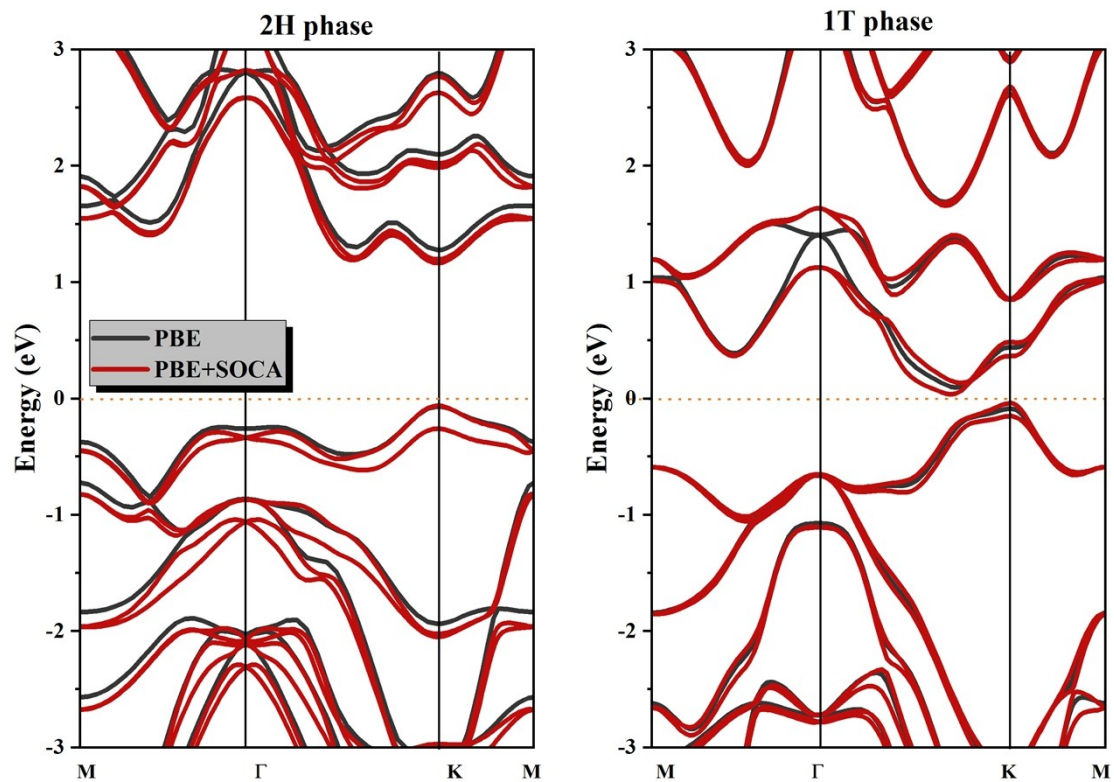


Figure. S6 Band structure of Janus MoSeTe monolayer in (a) 2H and (b) 1T phase, respectively, by using PBE (black solid lines) and PBE+SOC (red solid lines) functions, respectively. The dotted lines indicate the position of the Fermi level.

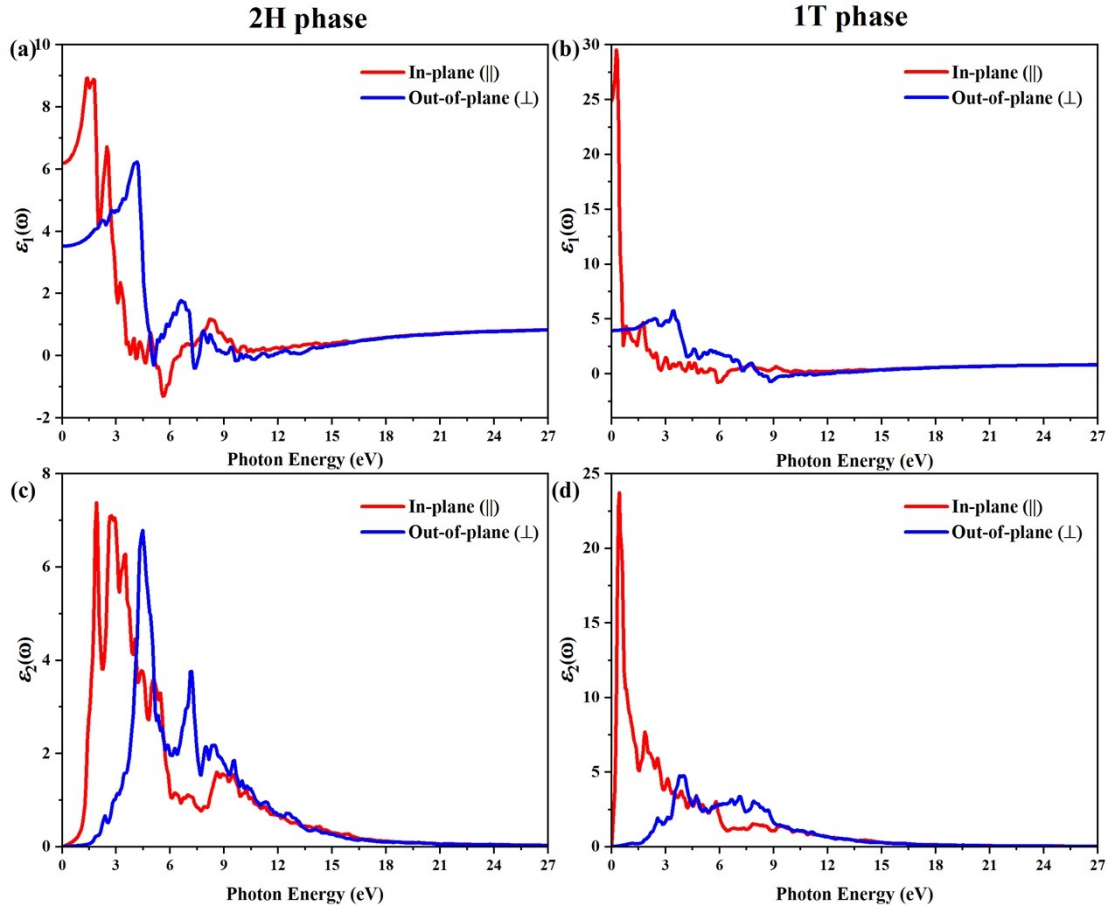


Figure. S7 The dynamical dielectric function $\epsilon(\omega)=\epsilon_1(\omega)+\epsilon_2(\omega)$ as a function of the photon energy for Janus MoSeTe monolayer in 2H phase (left) and 1T phase (right) obtained by PBE functional.

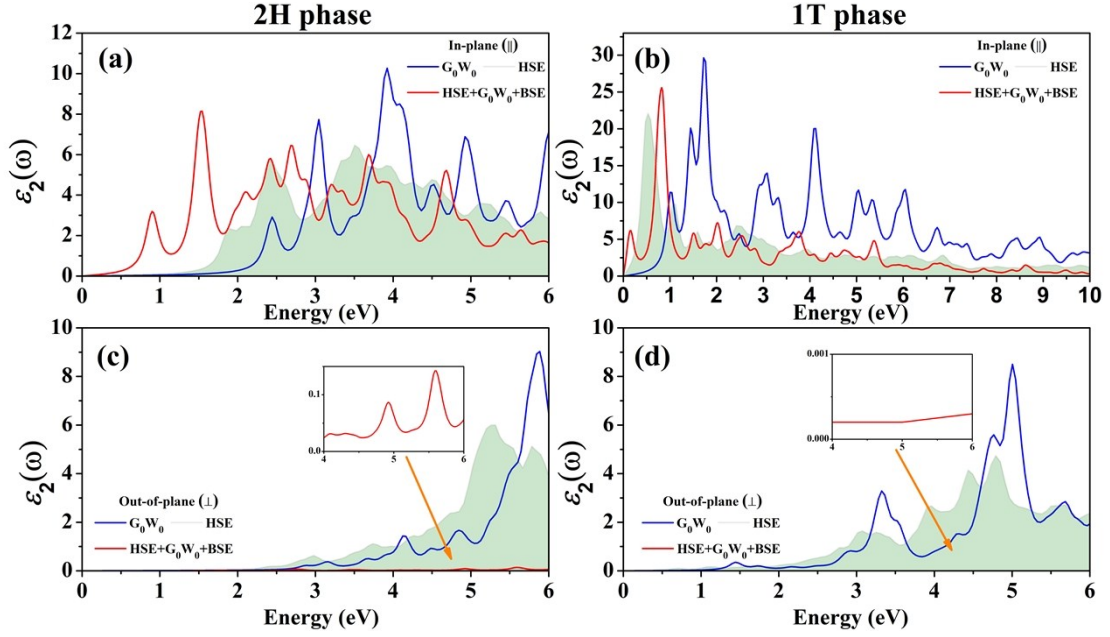


Figure. S8 The imaginary part of the dielectric function ε_2^{xx} and ε_2^{zz} corresponding to the (a,c) 2H and (b,d) 1T phases of MoSeTe monolayer along the x and z directions, respectively. The blue, gray and red solid lines represent the imaginary components calculated by using G_0W_0 , HSE06 and HSE+ G_0W_0 +BSE functions, respectively.

The imaginary part $\varepsilon_2(\omega)$ of dielectric function for Janus MoSeTe are also calculated at G_0W_0 level ($e-e$ correlation included and $e-h$ correlation neglected). Moreover, plus Bethe-Salpeter equation (BSE) introduces higher order interaction diagrams, i.e., both $e-e$ and $e-h$ effects which improves the electronic description systematically on top of G_0W_0 [1,2]. Thus, HSE+ G_0W_0 +BSE method was also considered. Here, $e-e$ and $e-h$ represent electron-electron and electron-hole correlations effects, respectively. The obtained results are collected in Fig. S8. From G_0W_0 and HSE+ G_0W_0 +BSE curves it is clear that the optical anisotropy between ε_2^{xx} and ε_2^{zz} largely increases by the inclusion of local field effects, as shown in Fig. S8(a) *Vs.* S8(c) or S8(b) *Vs.* S8(d). Additionally, the $e-h$ interaction produces mainly a renormalization of the intensity of the optical peaks calculated by G_0W_0 and HSE+ G_0W_0 +BSE methods. More inspecting the imaginary part of the dielectric function obtained at the HSE and G_0W_0 levels for both phases, one can see that the inclusion of the $e-e$ interaction leads to a blue shift. However, inclusion of both $e-e$ and $e-h$ interactions yields a significant red shift of $\varepsilon_2(\omega)$, which agrees with the previous results [3-5]. Another appealing peculiarity result is that the first BSE optical peak is in much better agreement with the electronic gap than other two calculated values, implying the weakly-bound excitonic/free carrier nature of the optical excitation. Therefore, the physical effect of $e-e$ and $e-h$ interactions (excitonic effects), reproduced by G_0W_0 +BSE, gives a more precise result. However, the total computation by G_0W_0 +BSE is much more expensive than other methods. More important, it is worthy to mention that the global shape of the spectrum are preserved calculated by these three methods for both 2H and 1T phases of MoSeTe monolayer. Comprehensive above factors, we conclude that optical

properties of Janus MoSeTe can be explained well by independent-particle transitions.

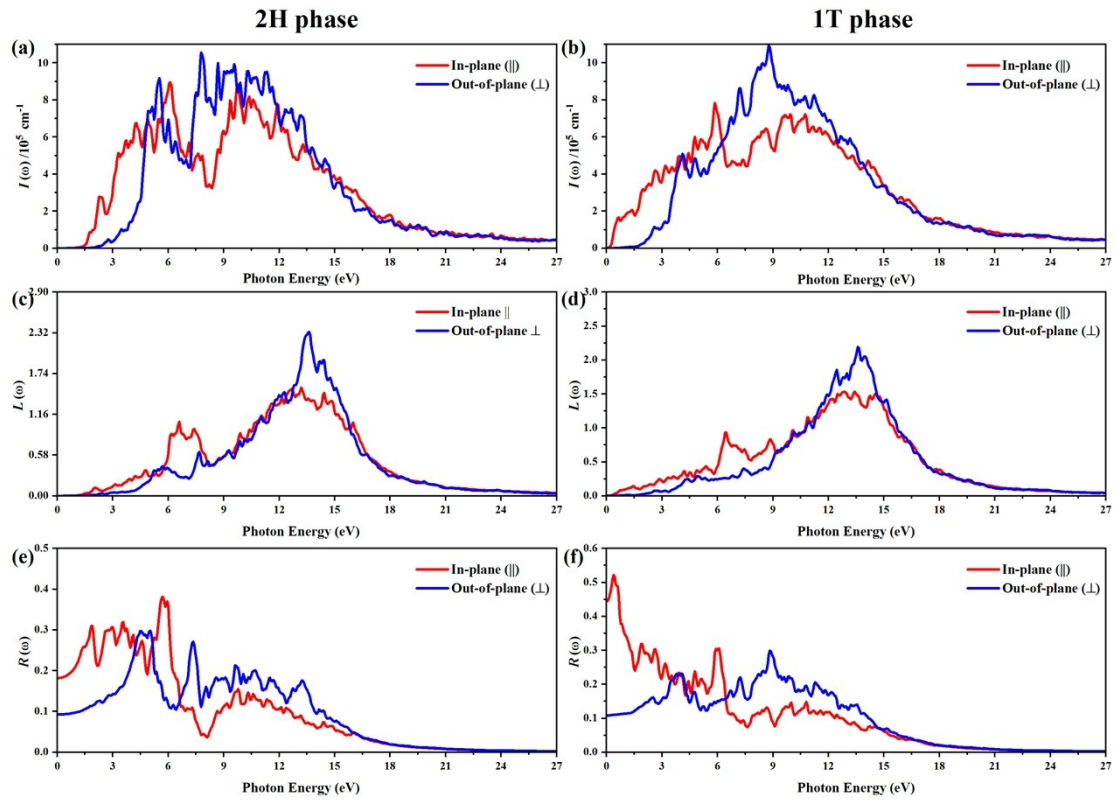


Figure. S9 Calculated absorption coefficient $I(\omega)$, energy loss spectrum $L(\omega)$ and reflectivity $R(\omega)$ for Janus MoSeTe monolayer in 2H phase (left) and 1T phase (right) obtained by PBE functional.

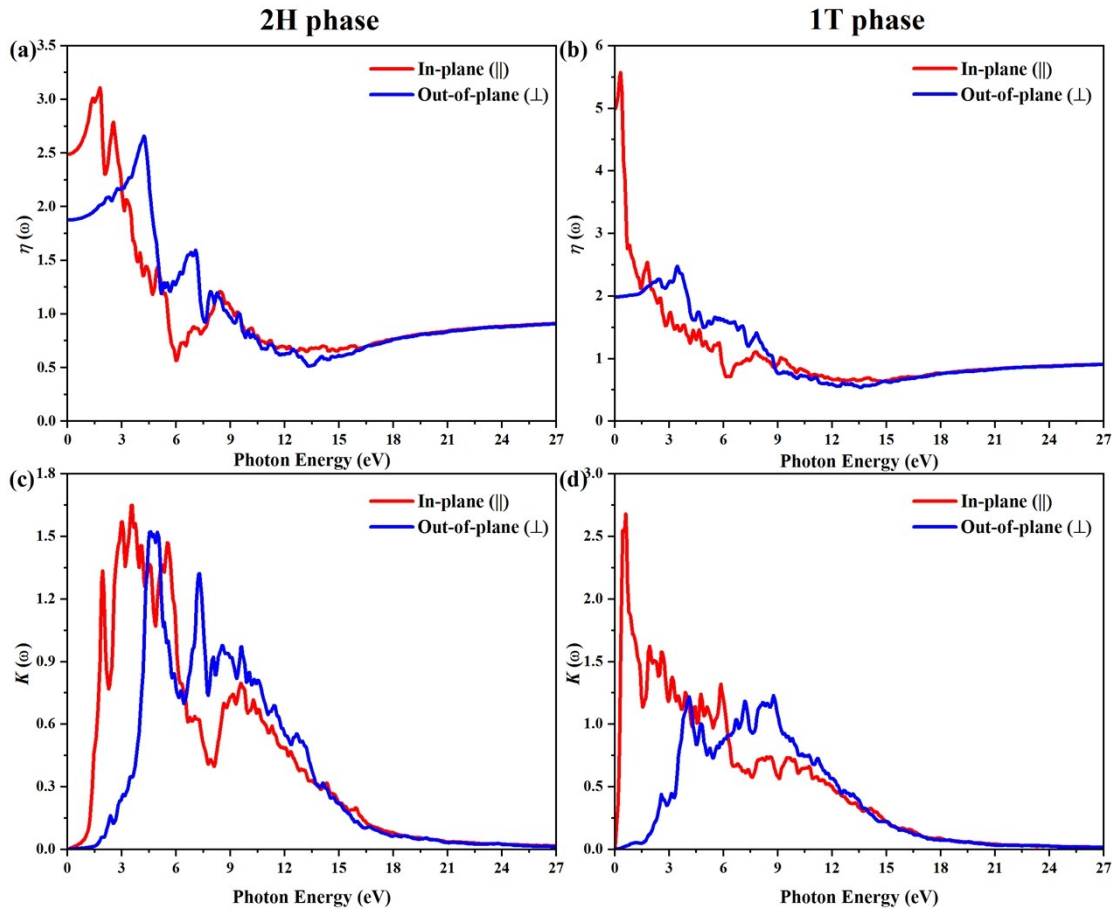


Figure. S10 Calculated refractive index $\eta(\omega)$ and extinction coefficient $K(\omega)$ for Janus MoSeTe monolayer in 2H phase (left) and 1T phase (right) obtained by PBE functional.

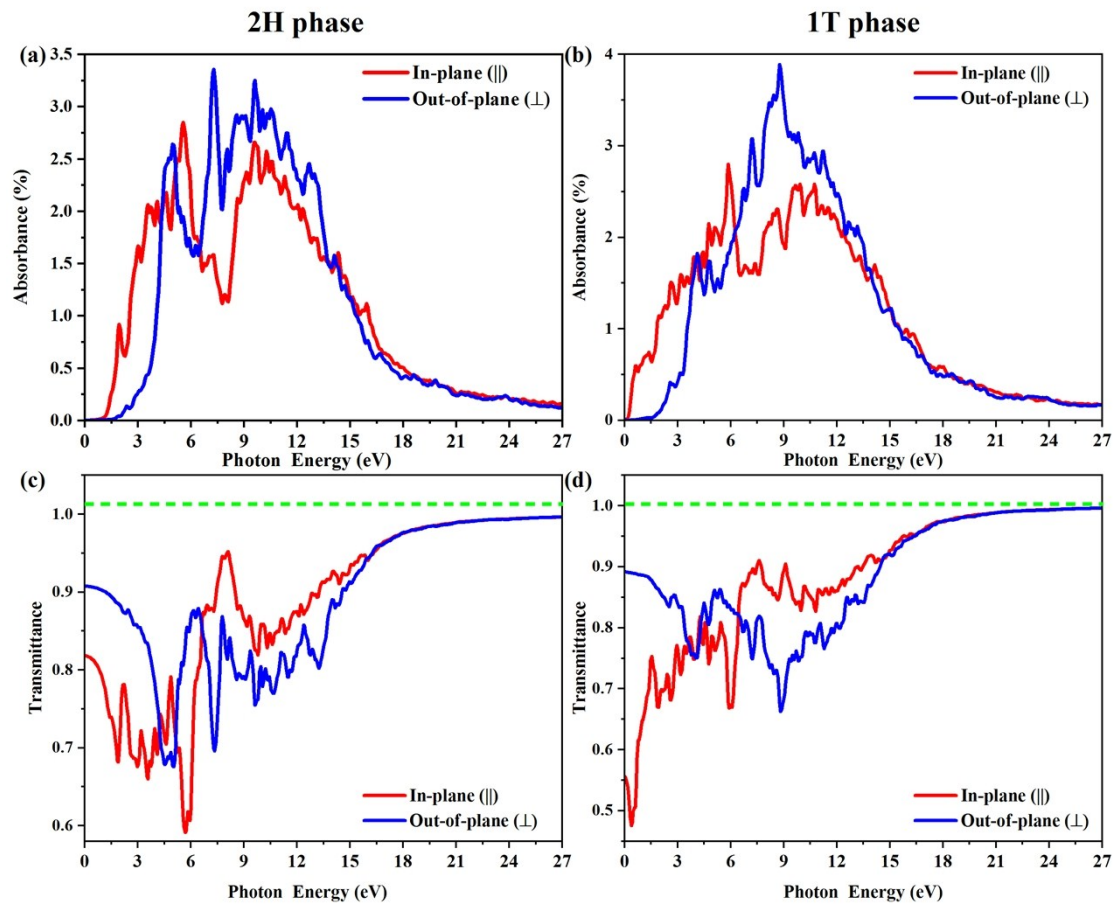


Figure. S11 Calculated absorbance and transmission spectrum for Janus MoSeTe monolayer in 2H phase (left) and 1T phase (right) obtained by PBE functional.

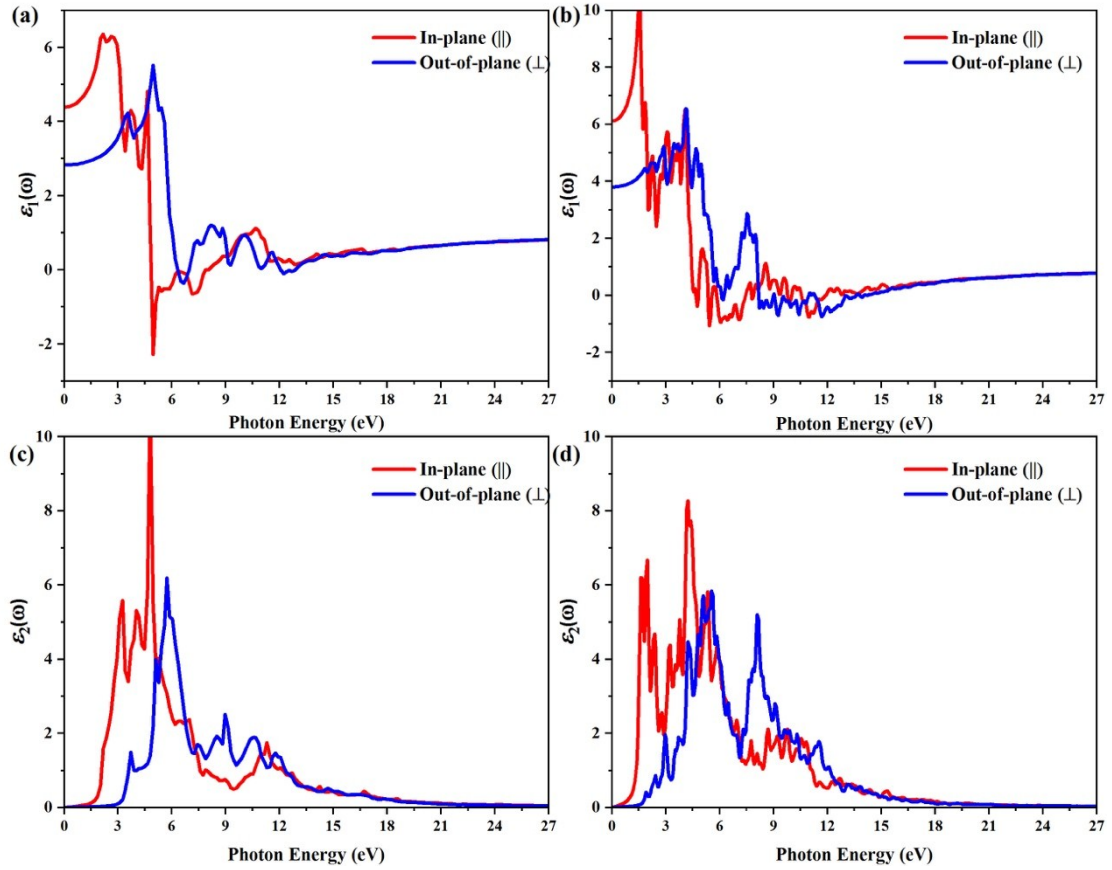


Figure. S12 The dynamical dielectric function $\epsilon(\omega)=\epsilon_1(\omega)+\epsilon_2(\omega)$ as a function of the photon energy for MoSe₂ (left) and MoTe₂ (right) obtained by HSE06 functional.

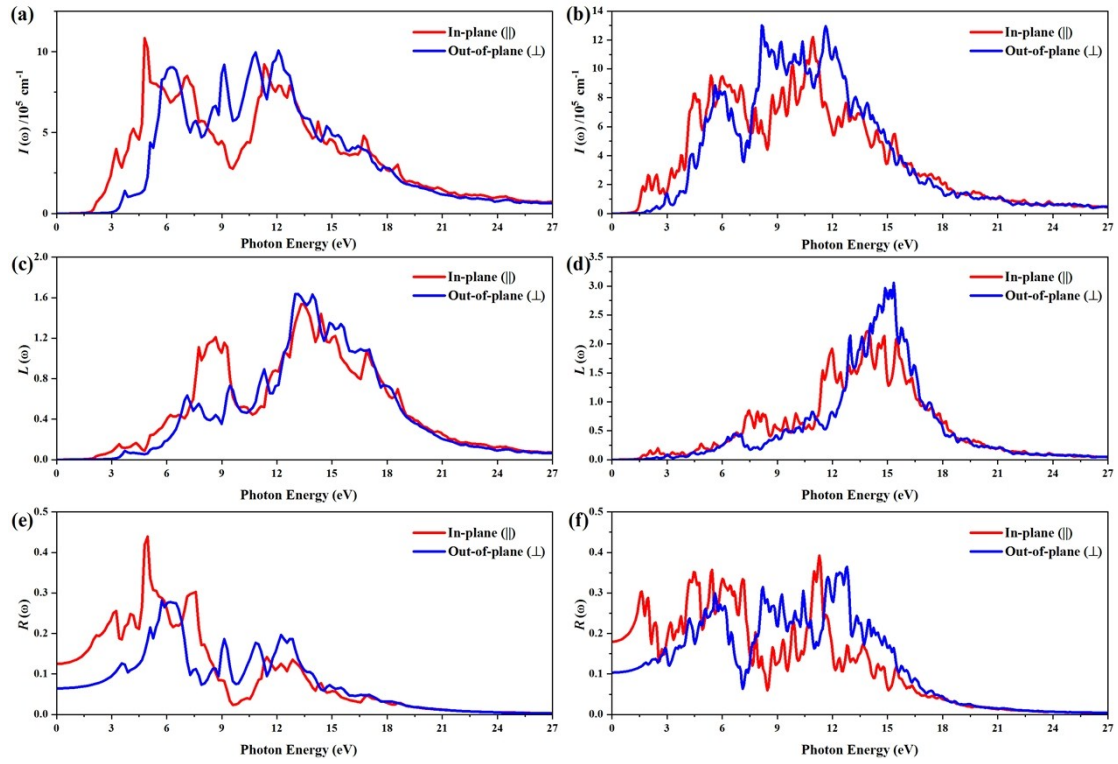


Figure. S13 Calculated absorption coefficient $I(\omega)$, energy loss spectrum $L(\omega)$ and reflectivity $R(\omega)$ for MoSe₂ (left) and MoTe₂ (right) obtained by HSE06 functional.

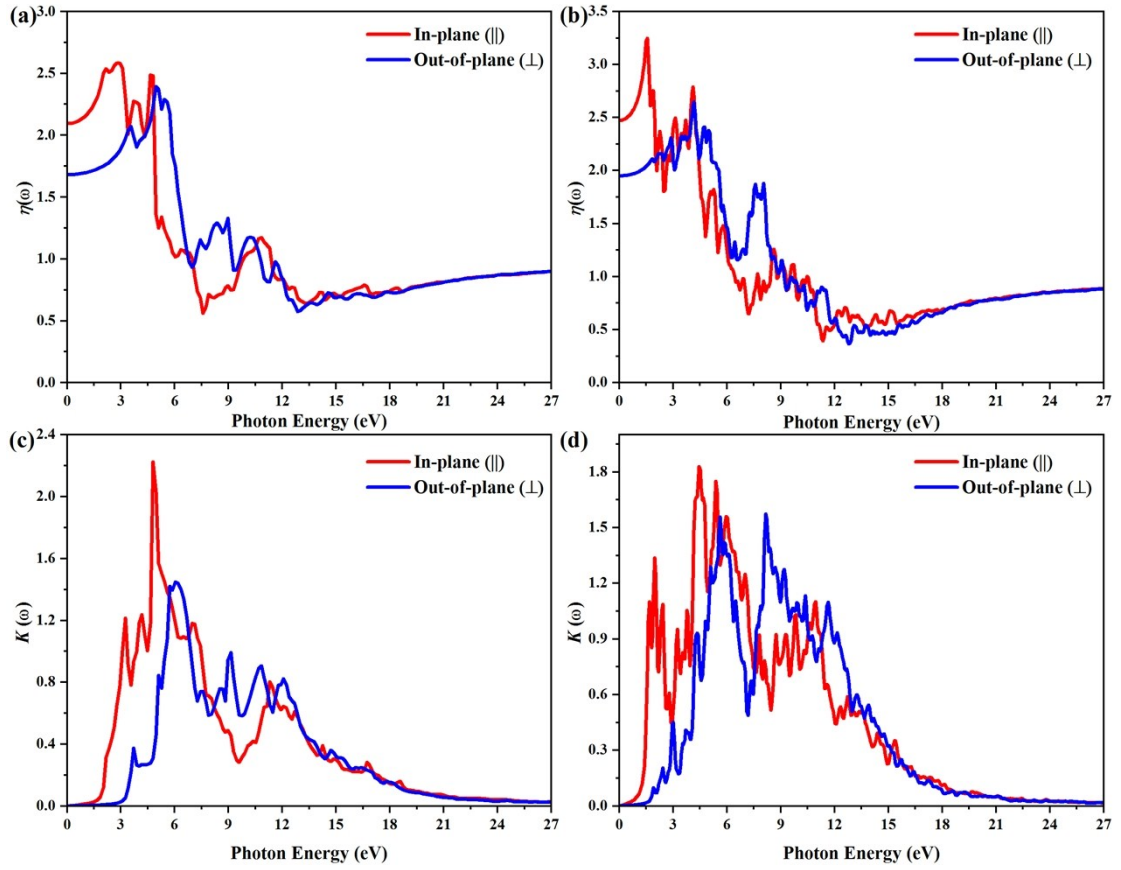


Figure. S14 Calculated refractive index $\eta(\omega)$ and extinction coefficient $K(\omega)$ for MoSe_2 (left) and MoTe_2 (right) obtained by HSE06 functional.

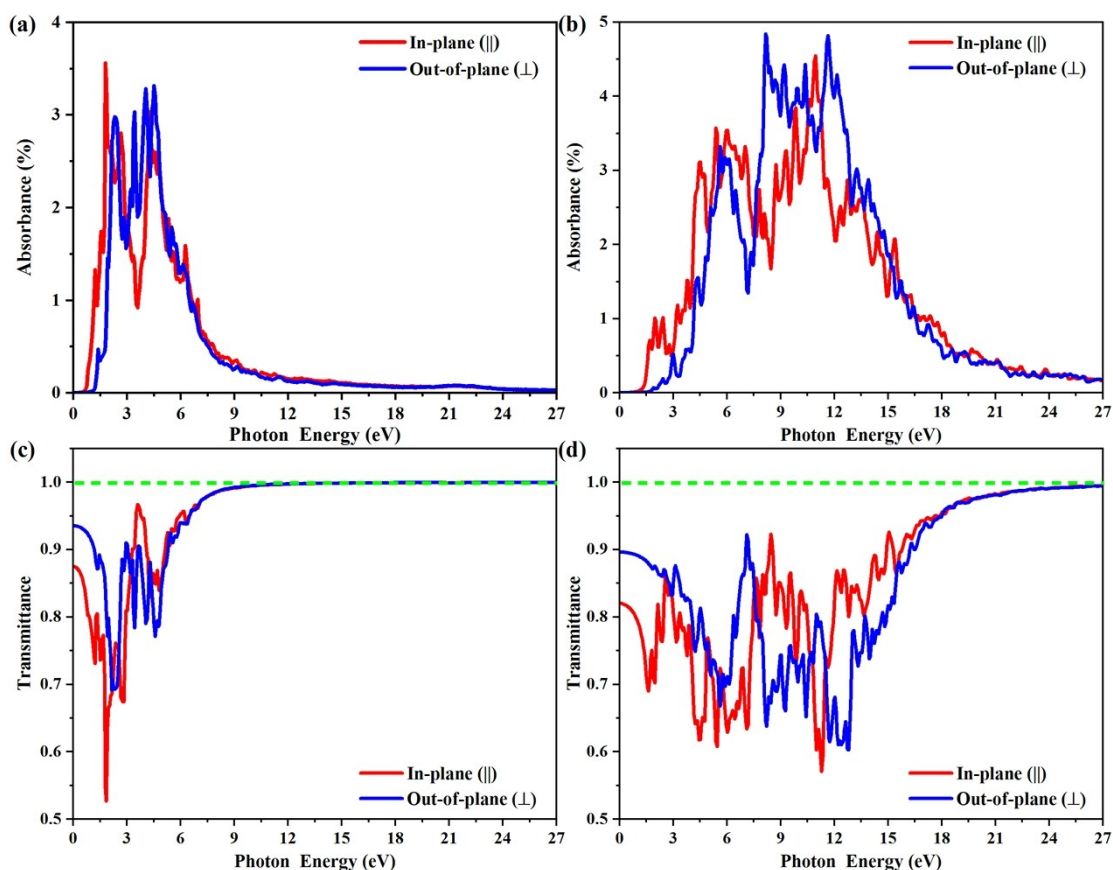


Figure. S15 Calculated absorbance and transmission spectrum for MoSe₂ (left) and MoTe₂ (right) obtained by HSE06 functional.

References:

- [1] Rohlfing, M.; Louie, S. G. Electron-Hole Excitations in Semiconductors and Insulators. *Phys. Rev. Lett.* 1998, 81, 2312.
- [2] Kresse, G.; Furthmüller, J. Efficiency of Ab-Initio Total Energy Calculations for Metals and Semiconductors Using a Plane-Wave Basis Set. *Comput. Mater. Sci.* 1996, 6, 15.
- [3] Guan, Z.; Ni, S.; Hu, S, Tunable Electronic and Optical Properties of Monolayer and Multilayer Janus MoSSe as a Photocatalyst for Solar Water Splitting: A First-Principles Study. *J. Phys. Chem. C* 2018, 122, 6209–6216.
- [4] F. Karlicky, M. Otyepka, Band gaps and optical spectra of chlorographene and graphane from G_0W_0 , G_0W_0 and GW calculations on top of PBE and HSE06 orbitals, *J. Chem. Theory. Comput.*, 2013, 9, 4155-4164.
- [5] Jin, H.; Wang, T.; Gong, Z.R.; Long, C.; Dai, Y., Prediction of an extremely long exciton lifetime in a Janus-MoSTe monolayer. *Nanoscale*, 2018, 10, 19310.